Domain switching in process zones of PZT: characterization by microdiffraction and fracture mechanical methods

Stefan Hackemann[a], Wulf Pfeiffer[b],*

[a]German Aerospace Center (DLR), Institute for Materials Research, Linder Höhe, 51170 Köln, Germany
[b]Fraunhofer-Institute For Mechanics of Materials (IWM), Woehlerstr. 11-13, 79108 Freiburg, Germany

Abstract

Ferroelastic domain switching in the vicinity of cracks in Soft-PZT was examined by X-ray microdiffraction. Preliminary experiments under electrical and mechanical load proved the ability of the method to quantitatively characterize domain switching in the process zone of cracks with sufficient local resolution. Using an in situ bending device the observation of domain switching under load was possible. The width of the process zone at a growing crack, measured by microdiffraction can be correlated with the increase of the crack resistance curve measured in fracture mechanical tests. The separation of mechanical and ferroelastic contributions to the R-curves was performed by determining R-curves before and after unloading the samples. Residual stresses caused by domain switching could not be detected. © 2002 Elsevier Science Ltd. All rights reserved.

Keywords: Domain switching; Ferroelastic properties; PZT; R-curves; X-ray methods

1. Introduction

The lifetime of ferroelastic based piezo-ceramic actuators is determined by crack propagation. Crack growth in ferroelastic/ferroelectric materials is influenced by domain switching, which is not considered by the common fracture mechanics. Similar to the stress induced transformation toughening in zirconia, domain switching reduces the local stresses at the crack tip, i.e. it causes partial shielding of the crack tip. Domain switching, like any other change in texture, and possibly associated residual stresses can be detected in crystalline materials by X-ray diffraction (XRD). Numerous papers deal with ferroelectric domain switching under electric fields[1–5] or ferroelastic switching under mechanical load.[6] The aim of the present investigation is the quantitative characterization of the process zone size and the amount of domain switching in a commercial tetragonal Soft-PZT (PIC 151, PI Ceramics, Germany) using micro-XRD techniques and fracture mechanical methods.

2. Experimental set-up

The microdiffraction system shown in Fig. 1 is equipped with a rotating anode as a radiation source with a maximum power of 18 kW, depending on the target material and the focus size. Pinhole collimators with a diameter of 0.05–0.8 mm and a 0.1 mm glass capillary for higher primary intensities and reduced exposure times determine the size of the primary beam. The sample on the xyz-stage can be observed and adjusted by a video microscope and a focussed laser. The diffracted intensity is counted by a two-dimensional position sensitive area detector with an active entrance window of 115 mm diameter.

Since tetragonal PZT is polarized along the crystallographic c-axis, only 90 and 180° switching can occur. Reflections of (002) and (200) lattice plains are suitable for the characterization of tetragonal 90° domain switching. Fig. 2 shows a switching process from a unit cell with the c-axis perpendicular to the sample surface into a orientation parallel to the surface plain. The diffraction pattern shows a loss of intensity of the (002)-reflection whereas the (200)-intensity increases.

The quantity $\Delta\iota$ which characterizes the amount of 90° domain switching is the change in the intensity ratio $I_{(002)}/I_{(200)}$:

$$\Delta\iota := \frac{\left(\dfrac{I_{002}}{I_{200}}\right)_{\text{load}} - \left(\dfrac{I_{002}}{I_{200}}\right)_{\text{init}}}{\left(\dfrac{I_{002}}{I_{200}}\right)_{\text{init}}}$$

Residual stresses of 1st order are investigated using the $\sin^2(\psi)$-method. The determination of stresses is based on the measurement of strain components $\varepsilon_{\varphi,\psi}$ as a function of the measurement directions φ,ψ and the use of the X-ray elastic constants $1/2\,s_2$ and s_1:

$$\varepsilon_{\phi,\psi} = (d_{\phi,\psi} - d_0)/d_0 = \tfrac{1}{2}s_2\sigma_\phi\sin^2\psi + s_1(\sigma_{11} + \sigma_{22})$$

with d_0 = unstressed lattice spacing, $d_{\phi,\psi}$ = measured lattice spacing, $\varepsilon_{\phi,\psi}$ = strain, ψ = tilt angle between normal on the lattice plane and normal on the sample surface, ϕ = direction of analyzed stress component σ_ϕ, and $1/2\,s_2 = (1+\nu)/E$, $s_1 = -\nu/E$ (E = Young's modulus, ν = Poisson ratio).
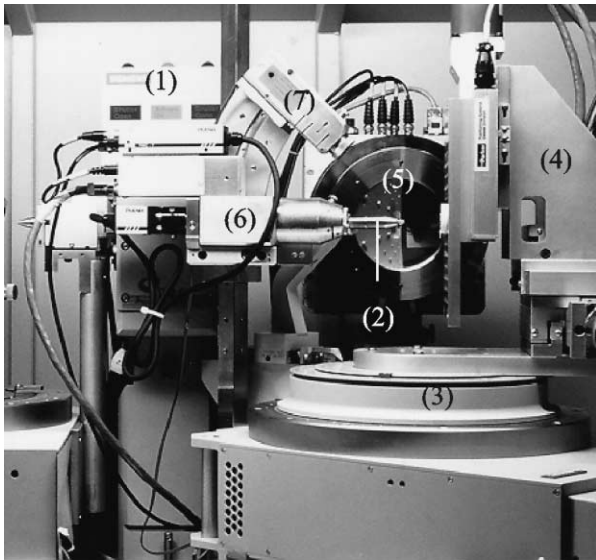

Fig. 1. Microdiffraction system (Bruker-axs), (1) rotating anode, (2) collimator, (3) goniometer, (4) xyz-stage, (5) area detector, (6) video camera, (7) laser.

The macroscopic elastic constants E and ν do not consider the anisotropy of the crystals and the coupling conditions between the crystallites. For reliable stress measurement s_1 and $1/2\,s_2$ respectively E^{XRD} and ν^{XRD} can be determined experimentally or calculated on the basis of the single crystal constants of elasticity.

The local resolution is mainly limited by the absorption and the grain size of the material. The irradiated volume is defined by the spot size of the X-ray beam and its penetration depth, while the number of crystallites or domains is determined by the irradiated volume and the grain size. Small spot sizes cause a dissolution of an homogeneous diffraction cone into single reflections. The remaining information can not be assumed as statistically relevant any more. The local resolution can be improved by rotations of the sample during the exposure. A rotation of 180° with respect to the ϕ-axis (which is perpendicular to the sample surface) in combination with an integration along the diffraction cone registered by the area detector optimizes the grain statistics. For the (002)/(200) reflections an aperture diameter of 0.1 mm was the limit for the investigated Soft-PZT PIC 151 with a grain size of 6 μm. Smaller grain sizes would permit a higher local resolution, but the rise of R-curves and the process zone size would decrease with the grain size.[7]

A special four point bending device was developed (see Fig. 3) which allows free access of the X-ray beam on the sample surface during a full 180°-rotation and for a diffraction angle 2θ of 45°. Sample dimensions were $25\times4\times3$ mm with respect to the limited space inside the microdiffraction system.

Stress intensity factors K_{I} were calculated as follows[8]

$$K_{\text{I}} = \frac{F}{B\sqrt{W}}\frac{S_1 - S_2}{W} \cdot \frac{3\Gamma\sqrt{\alpha}}{2\cdot(1-\alpha)^{3/2}}$$

with

$$\Gamma = 1.9887 - 1.326\alpha - \frac{(3.49 - 0.68\alpha + 1.35\alpha^2)\alpha(1-\alpha)}{(1+\alpha)^2}$$

and F = force, S_1, S_2 = distance of the rollers, B = sample width, W = sample height, a = crack length and $\alpha = a/W$.

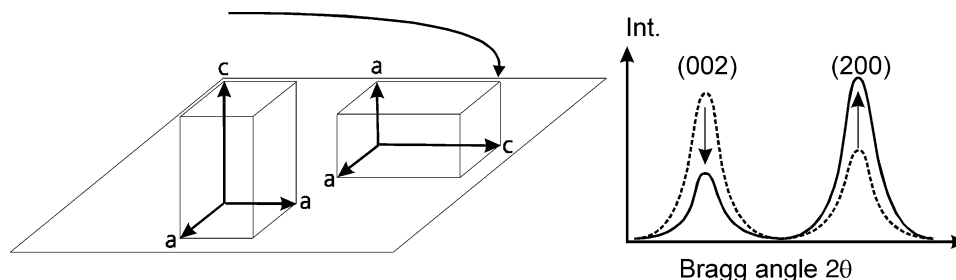The crack tip position was determined with an optical microscope. The accuracy of the determined crack tip

Fig. 2. Switching process and effect on diffraction pattern.

position was 5 μm, the accuracy of the load cell 1.5%. The R-curves had a statistical error of 2.5%.

3. Results

3.1. Domain switching due to an electric field

The crystallites of the investigated Material PIC 151 have a tetragonal unit cell with the following parameters:

$$c = 4.1048 \pm 0.0014 \text{ Å}, \ a_1 = a_2 = 4.0427 \pm 0.0017 \text{ Å},$$
$$\alpha = \beta = \gamma = 90° \text{ and } c/a = 1.0154 \pm 0.0005$$

Similar to the common "butterfly curves" which show the strain caused by domain switching processes as a function of the applied electric field, the intensity ratio $I_{(002)}/I_{(200)}$ as a function of the electric field E also should have a "butterfly-shape". Fig. 4 shows the XRD-butterfly curve determined at the flat electrode surface of a cylindrical sample (10 mm diameter, 1 mm thickness). The changes in the intensity ratio are distinct, the coercitive field E_c is about 7 kV/cm, taken from the minima of the 1st and 50th cycle.

The results of the measurements on the free surface adjacent to the electrode surfaces of a poled sample are illustrated in Fig. 5. Here, due to the observation direction transverse to the applied electric field and the poling direction, the inverse intensity ratio $I(200)/I(002)$ has to be plotted to obtain a butterfly curve. An electric field reverse to the poling direction was applied and slowly increased (Fig. 5: ①, ③), followed by long holding times and decreasing electric field (②,④).

Compared to the measurement on the electrode surface (Fig. 4), the butterfly-shape in Fig. 5 is less distinct. The intensity ratio shows smaller changes, i.e. less domain switching processes occur. The coercitive field, taken from the local minima, is apparently higher ($E_c = 10$ kV/cm) and a strong creep can be observed during the holding times on both "wing tips" of this butterfly-curve. Obviously domains at the sample surface adjacent to the electrodes follow slowly the switching processes occurring mainly inside the sample and are less affected by the electric field itself. Thus, the following investigations were performed at the electrode-surfaces.

3.2. Domain switching and plastic strain: mechanical loading

The measurement of domain switching under mechanical load (Figs. 6–8) was determined using a four-point bending device, which allows to investigate the tensile surface by XRD-experiments under load. The load was increased stepwise using a high loading speed,

the intensity ratio was measured 15 min after the desired load was adjusted.

The ferroelastic domain switching due to mechanical stress also resulted in distinct changes in the intensity ratio above a critical stress level of 15 MPa for domain switching (see Figs. 6 and 7). Increasing the mechanical loading up to 40 MPa reduced the intensity ratio $I(200)/I(002)$ to about 66% of the initial value. Surprisingly, the percentage of domain switching was similar for an unpoled sample and a sample poled perpendicular to the tensile loading stress, although the poling direction of the poled sample should increase the potential of domain switching processes.

The "plastic" strains (due to domain switching occurring during the loading experiment) and the changes in the intensity ratio show a linear dependence (see Fig. 8). The experiment was carried out as above with the four-point bending device and strain measurements (through a strain gauge) at the tensile surface. The plastic strain can be estimated as

$$\varepsilon_{\text{plast}} = \varepsilon_{\text{obs}} - \sigma/E$$

using $E = 60$ GPa.

The slope m of the regression line found in Fig. 8 is $1/m = (-3.3 \pm 0.2) \ 10^{-3}$.

Thus, the local plastic strains can be estimated by

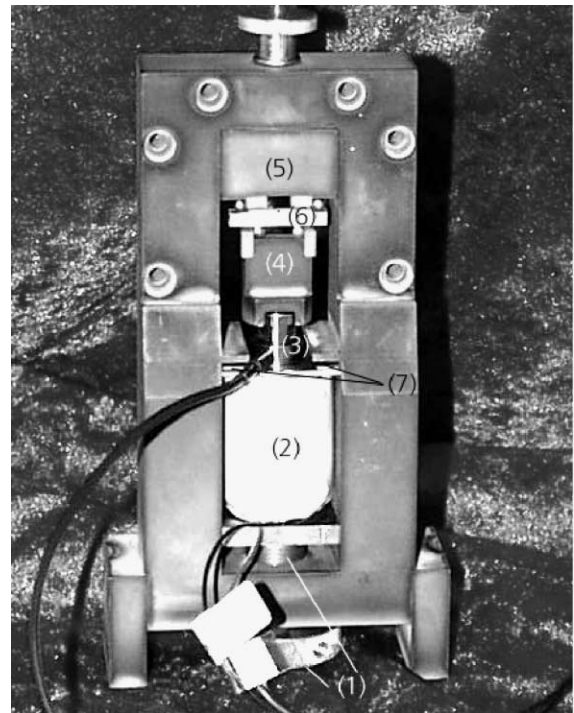$$\varepsilon_{\text{plast}} = 1/m \ \Delta\iota.$$

Fig. 3. Bending device, (1) pre-load screw, (2) piezo stack, (3) load cell, (4) lower and (5) upper bearing with magnets, (6) bending bar, (7) leaf spring.

3.3. Crack growth resistance

The samples were ground, polished and notched, the notch being finally sharpened using the razor blade method. Although the resulting notch radius was only about 0.015 mm, nearly the complete R-curve had been anticipated by the process zone of the notch (see the initial stress intensity factors in Fig. 9). Therefore the samples had to be additionally precracked and tempered for 24 h at 310 °C (which is 50 °C above T_{Curie}).

Fig. 10 shows the R-curves of five unpoled samples, the initial value is 0.49 MPa m$^{1/2}$, the R-curve reaches a plateau value of 0.88 MPa m$^{1/2}$ after a crack propagation of 400 μm.

Some samples were poled at electric fields of 30 kV/cm. The poling direction is perpendicular to the tensile stress to increase the potential of domain switching processes. Surprisingly, the poling had no strengthening effect on the R-curves, see Fig. 11.

After recording the R-curves some samples were completely unloaded and relaxed for 24 h. The samples were loaded again and new R-curves recorded (Fig. 12). The new initial values (0.53 MPa m$^{1/2}$) are only slightly higher than the first values. The rise distance is 200 μm and shorter than the first rise.

The time-consuming microdiffraction experiments under load (see below) were carried out at 50% of K_{IR} to avoid subcritical crack growth. Thus, additional
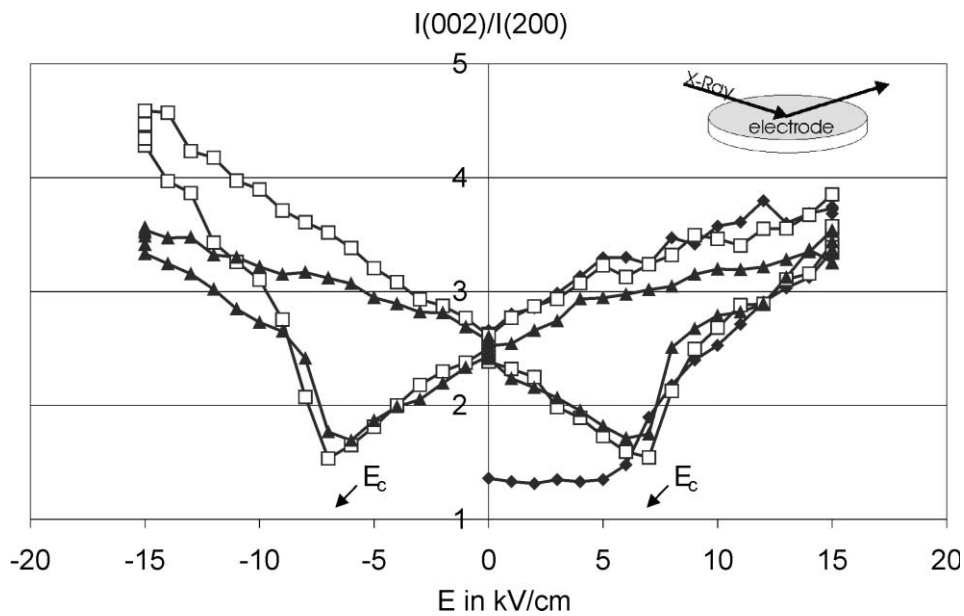

Fig. 4. Butterfly curve determined at the electrode surface, virgin curve (◆),1st cycle (□) and 50th cycle (▲).
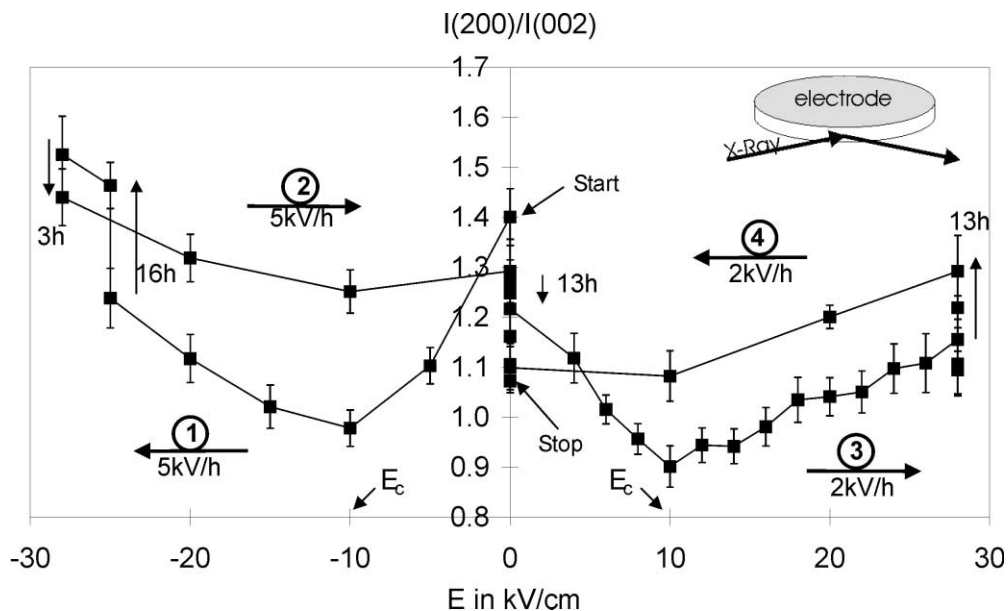

Fig. 5. Butterfly curve taken from the surface adjacent to the electrodes with holding times and time dependent change in the electric field.

continued R-curves after 15 h (the typical time needed for the XRD-measurements) at 50% of K_{IR} were recorded. Fig. 13 shows, that the new K_{IR} start values are about 72% of the plateau values and indicates, that the domains partially switch back during the XRD-analysis period.

3.4. Micro-XRD characterization of the process zone

The measurement of the domain switching in the vicinity of the cracks were conducted with poled and unpoled samples. As the poling did not significantly influence the process zone, only the results of the unpoled

samples will be shown here. Measurements were carried out using CuK_α radiation (45 kV/100 mA) and a 0.1 mm glass capillary under 180° ϕ-rotation in This results in circle shaped spots with a diameter 0.28 mm. The spots covered a area of 1.5×2.0 mm and had a distance of 0.1 mm to each other, so 336 overlapping spots covered the measurement area. The measurement time was 15 h. The samples were measured at three states:

1. precracked,
2. with crack partially unloaded to 50% of K_{Ic} to avoid subcritical crack growth,
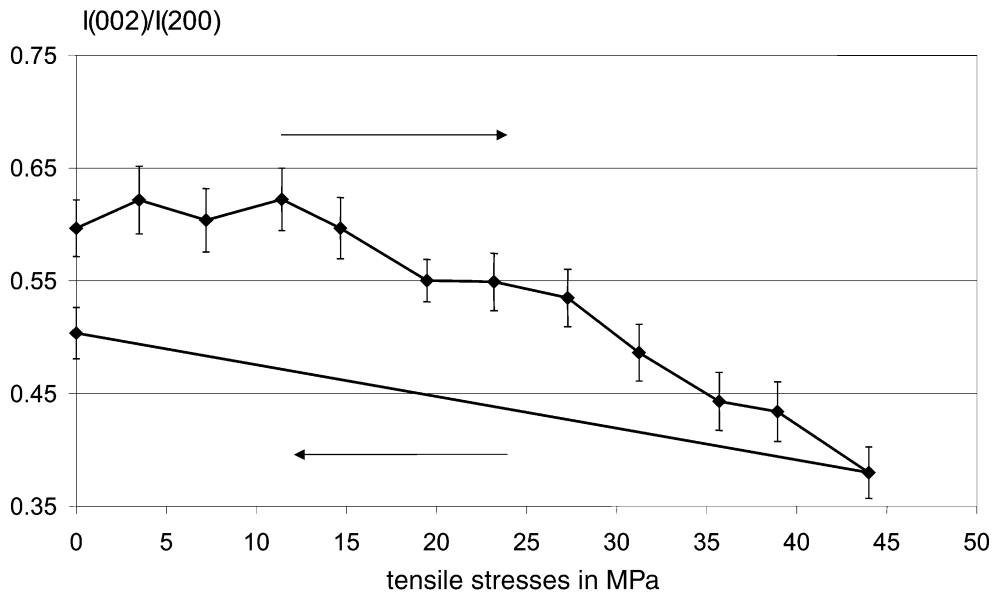3. unloaded.

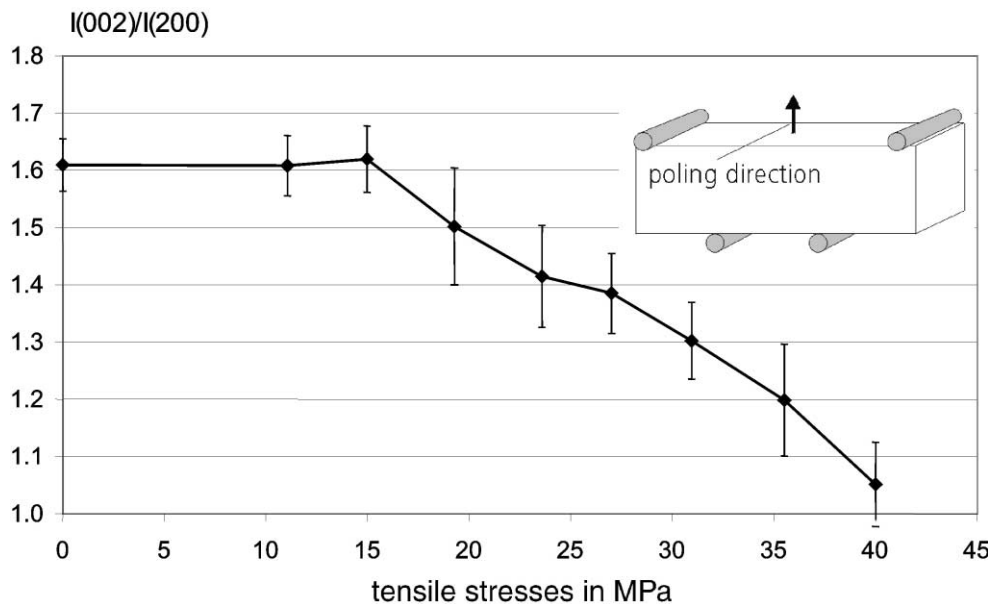Fig. 6. Intensity ratio as a function of tensile stresses (unpoled sample).

Fig. 7. Intensity ratio as a function of tensile stresses (poled sample).

The domain switching $\Delta\iota$ due to the separate processes, crack propagation, partially and complete unloading are then derived from two differences between the appropriate states. Negative $\Delta\iota$-values indicate a 90° switching of domains with the c-axis perpendicular to the surface into an orientation with the c-axis parallel to the surface.

Fig. 14 shows the domain switching caused by crack propagation plus the unloading to 50% of K_{Ic} (average of five unpoled samples). The corresponding R-curves of these samples are presented above. The most intense switching processes can be observed 200 μm behind the crack tip. Immediately behind the crack tip already a reorientation of domains due to the beginning contact of the partially unloaded contact occurred. This effect is more pronounced in Fig. 15.

In Fig. 16 the reorientation process caused by the complete unloading is illustrated. The strongest domain switching can be observed at the ligament at half the crack length. Domains with in-plane c-axis switch back into an orientation with the c-axis perpendicular to the surface.

Distinct remanent domain switching is presented in Fig. 16. The strongest switching processes concentrate to the middle section of the crack path. For the poled samples no stronger domain switching could be observed.

The process zone height h (transverse to the ligament) was calculated from the data presented in Fig. 14, observed 200 μm behind the crack tip ($y = 0.7$ mm), where the most intense switching processes could be detected. The measured distribution of $\Delta\iota$ actually is a
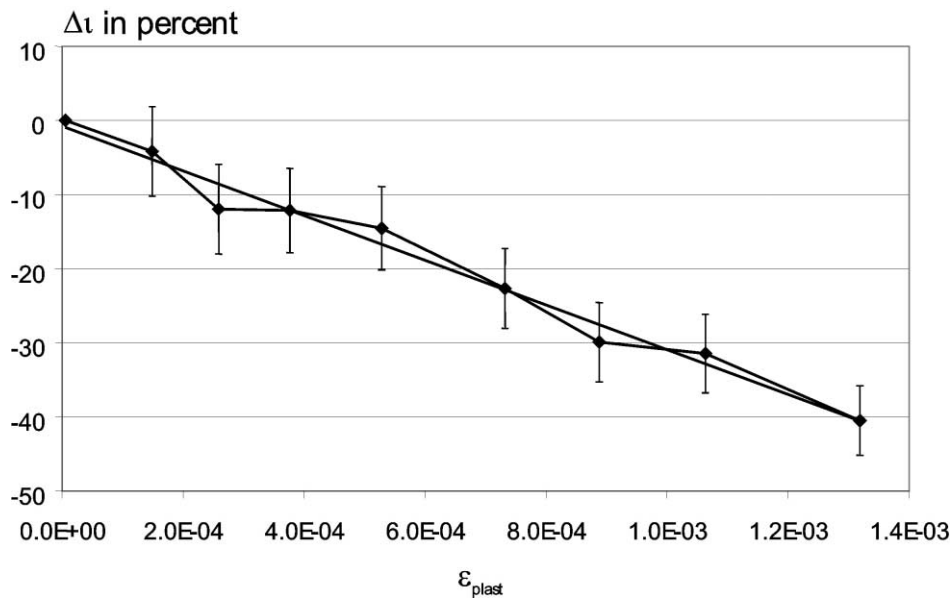

Fig. 8. Change in intensity ratio $\Delta\iota$ as a function of plastic strain (unpoled sample).
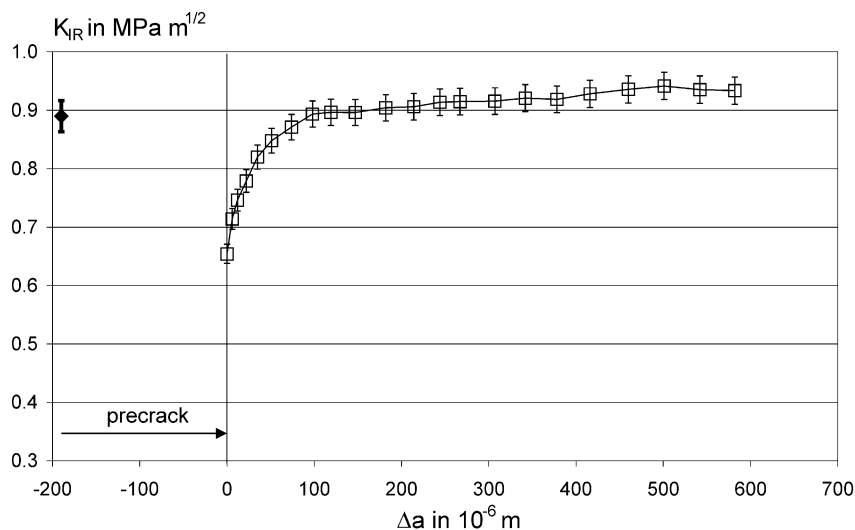

Fig. 9. Initial stress intensity factor of a notched specimen and R-curve after additionally pre-cracking and annealing of the sample.
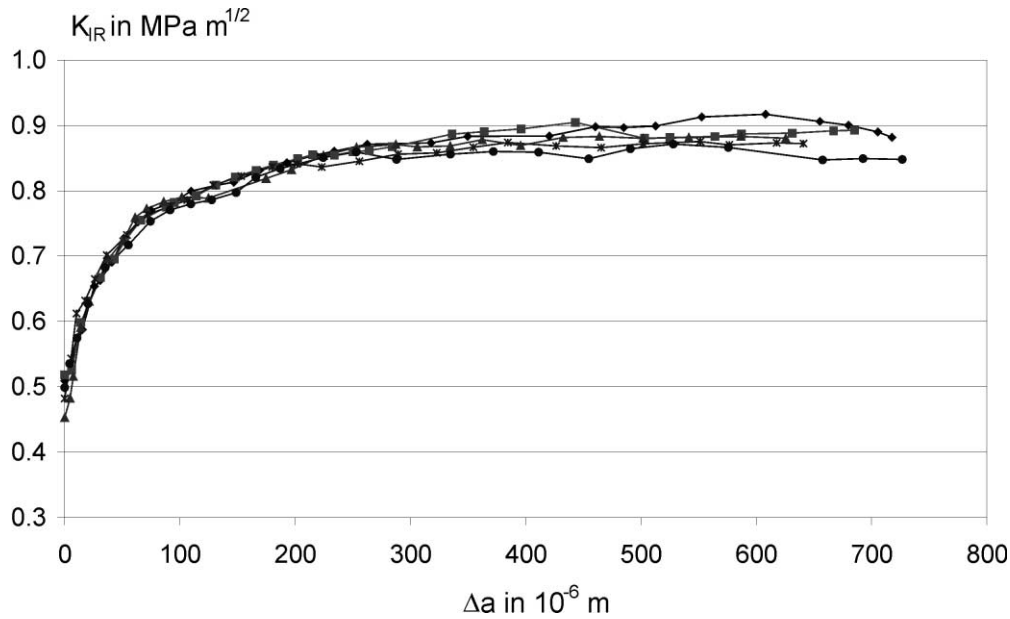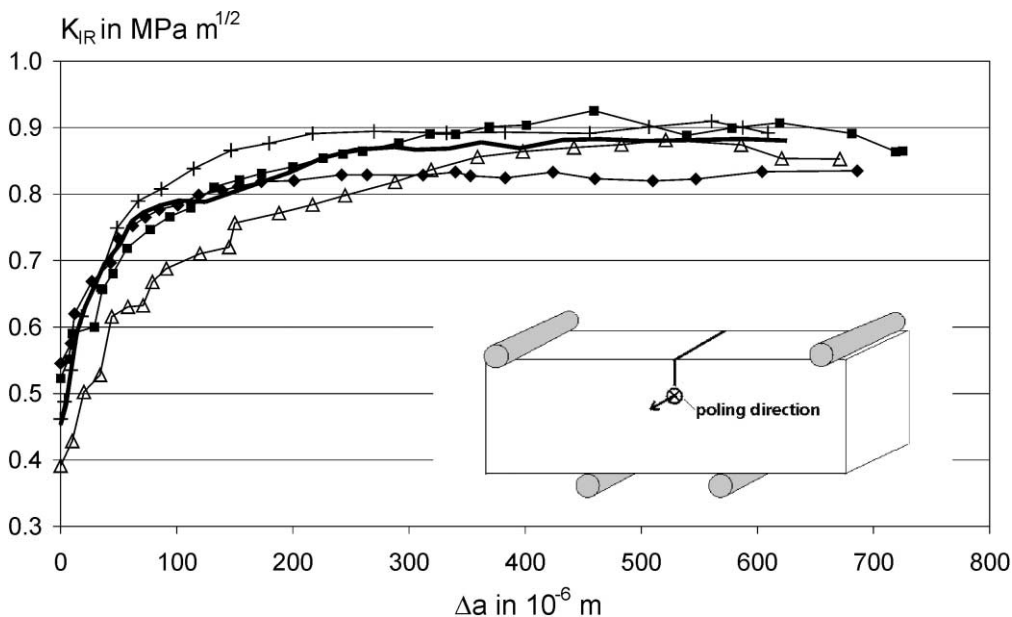
Fig. 10. R-curves of five unpoled samples.

Fig. 11. R-curve of four poled samples and an unpoled sample (fat line).

convolution of spot size, the distribution of the X-ray intensity in the primary beam (a Gaussian distribution was assumed) and the true distribution of the domain switching $\Delta\iota^\circ$. Fig. 17 shows, that the difference between measured distribution $\Delta\iota$ and deconvoluted distribution of $\Delta\iota^\circ$ is negligible. The "true" process zone height h in Fig. 17 can be calculated to 0.29 ± 0.05 mm and refers to the observed R-curve rise (Fig. 10), the crack tip speed (10^{-6}–10^{-7} m/s) and the sample dimensions.

Residual stresses were measured with a pinhole collimator of 0.3 mm. The measurement of each stress component took 2 h. Table 1 contains the residual stress of sample U-Da-2 in x-direction parallel to the tensile

stress and the preferred switching direction. No significant residual stresses could be detected.

Five more samples were analyzed in the area of the crack tip. As above, no residual stresses could be found.

4. Discussion and conclusions

The present studies are able to correlate domain switching processes and R-curve behavior. Experiments with a complete or partial unloading during evaluation of the R-curves show a loss in crack growth resistance. This can be explained by the partial degradation of the shielding effects to reverse domain switching processes.
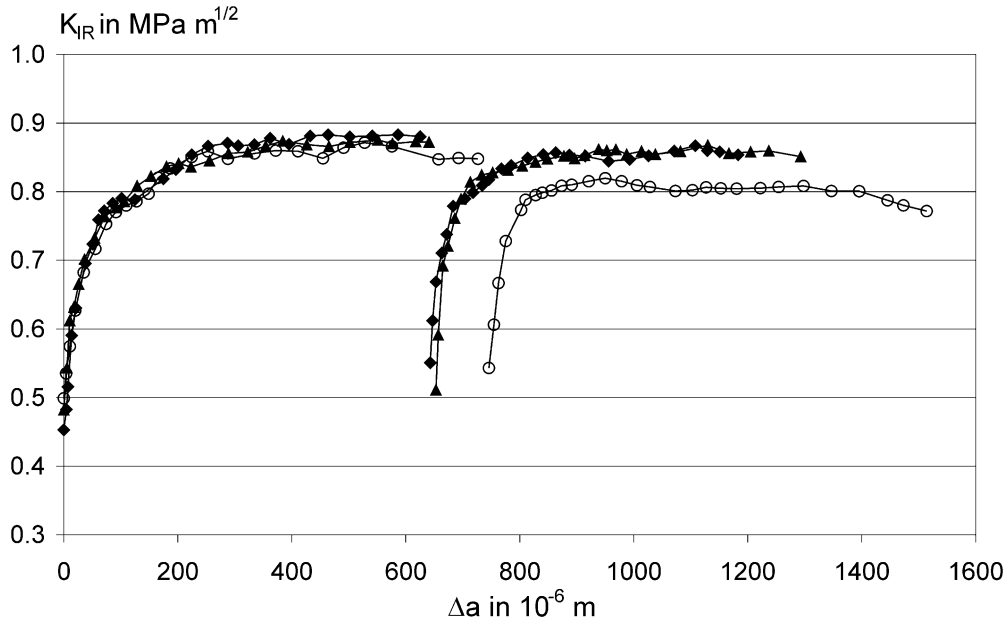
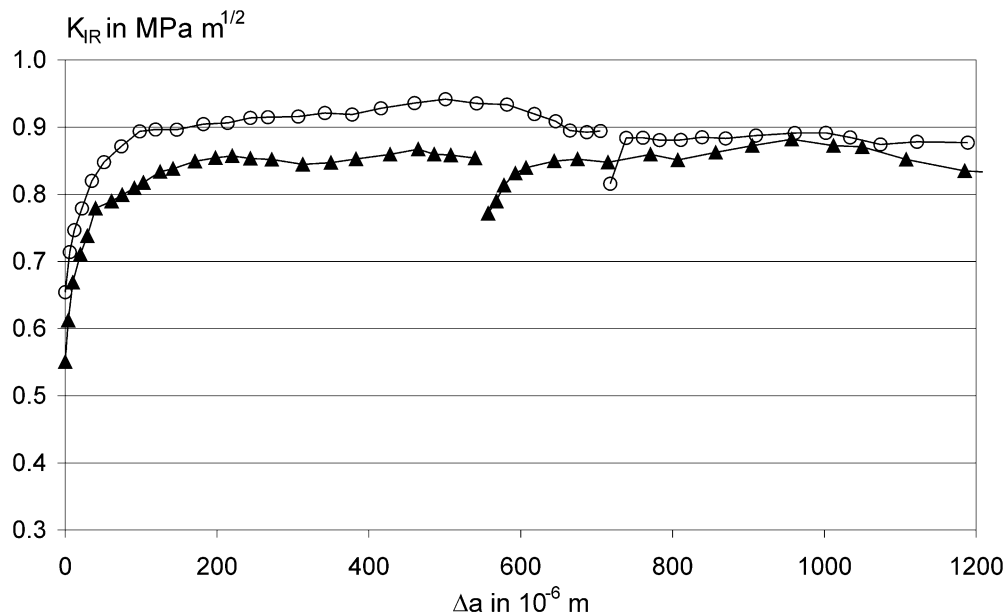Fig. 12. Continued R-curves after complete unloading.

Fig. 13. Original and continued R-curve after 15 h hold time with 50% load.

The rise of the R-curves is mainly based on ferroelastic domain switching processes. This can be concluded from Fig. 12, as other contributions to the crack growth resistance like micro-cracking, bridging or crack tip deflection are not reversible. The absence of strengthening effects by poling was not expected and is in contradiction to other studies. The observed $\Delta\iota$-values indicate that the domain switching processes are not even saturated for unpoled samples. Thus, an additional poling may not significantly increase the reservoir of domain switching processes and therefore also does not have a contribution to the R-curve behavior.

According to Evans[9] the rise of the crack growth resistance due to transformation toughening in ZrO$_2$-ceramics can be described as

$$\Delta G = V_f \int_{-h}^{h} \Delta U_I^C dx = 2V_f e^T \sigma_c h.$$

where ΔU_I^C is called the interaction energy, h the process zone height, V_f the transformed volume portion, e^T the transformation volume change and σ_C the critical transformation stress. The plastic strain by transformation toughening is described by ($V_f\, e^T$). An analogous
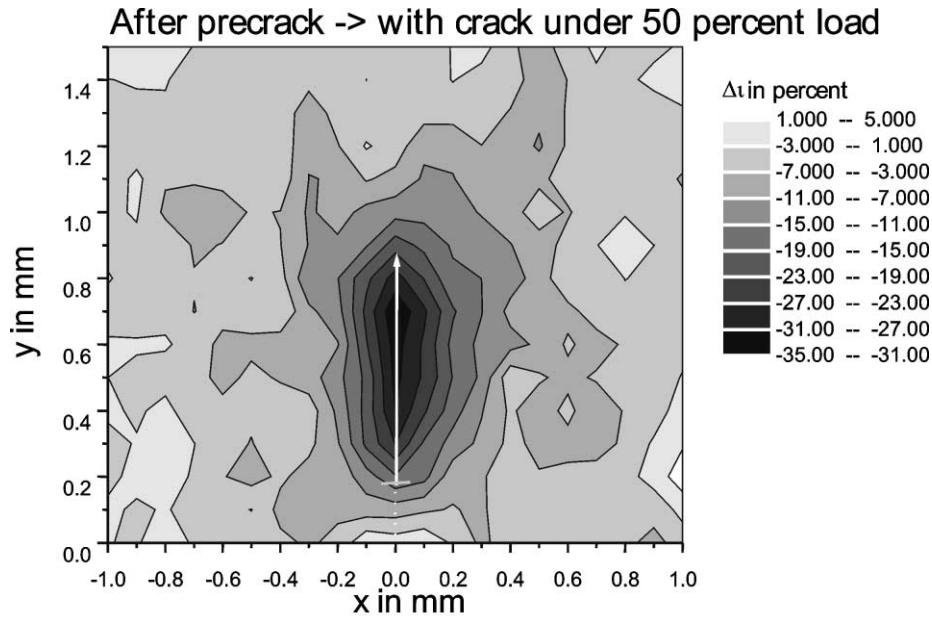
Fig. 14. Domain switching at the surface of unpoled samples caused by crack propagation plus partially unloading to 50% K_{Ic} (average of five unpoled samples, crack path shown as an arrow).
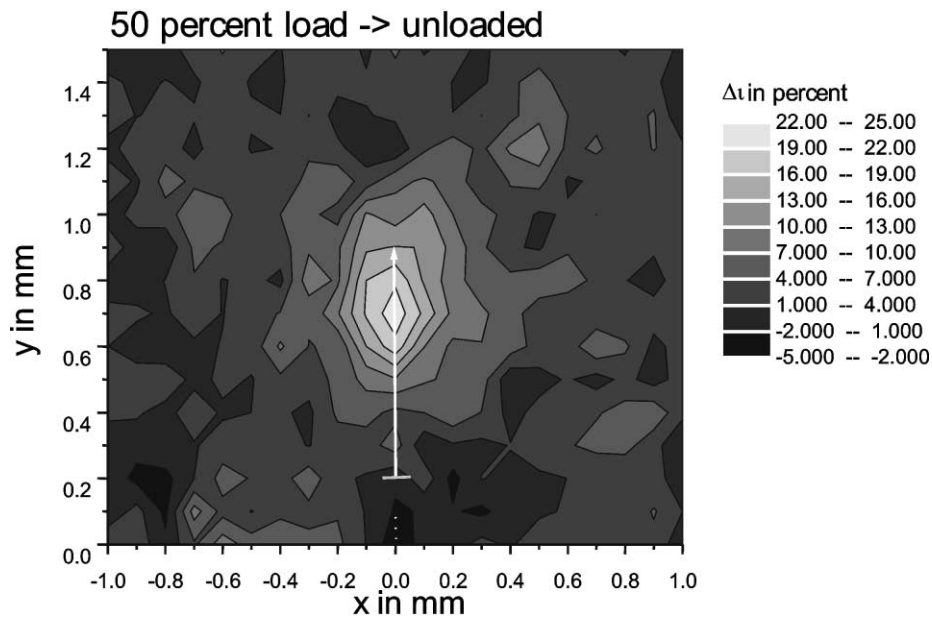

Fig. 15. Reorientation of domains at the surface of unpoled samples caused by unloading from 50% K_{Ic} to zero load (average of five samples, crack path shown as an arrow).

estimate for ferroelastic domain switching can be derived as followed:

$$\Delta G = 2\varepsilon_{pl}\sigma_c h,$$

where ε_{pl} is the plastic strain caused by domain switching.

The relationship

$$G_I = K_I^2 (1 - v^2)/E$$

leads to

$$\Delta K_I = K_{Ii}\left[\sqrt{1 + \frac{E\Delta G}{(1 - v^2)K_{Ii}^2}} - 1\right],$$

(K_{Ii} = initial value of the R-curve).

The plastic strain can be estimated from the correlation between the domain switching and plastic strain (see above) based on the strongest domain switching occurring
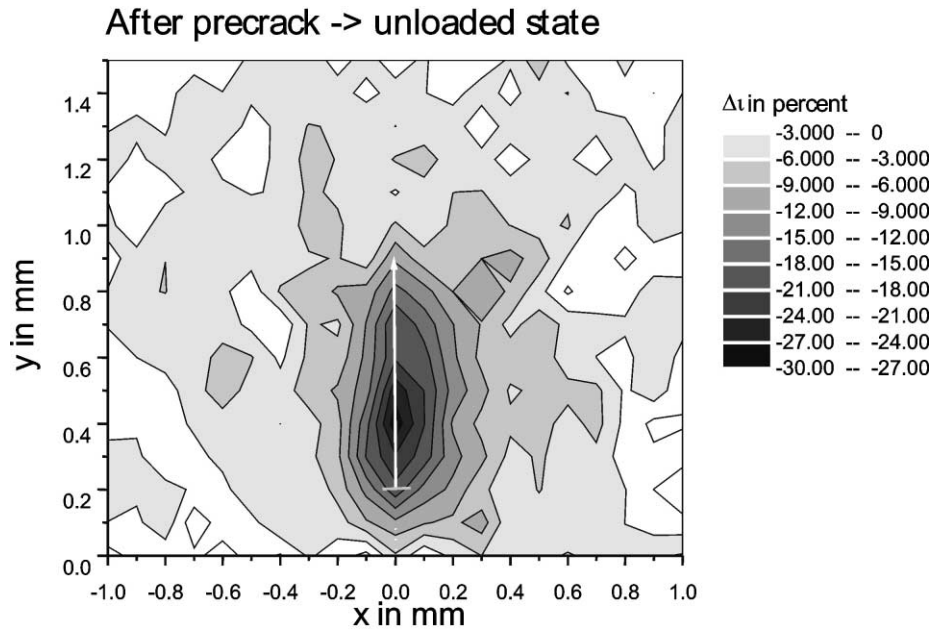
After precrack -> unloaded state

Fig. 16. Remanent domain switching at the surface of unloaded unpoled samples caused by crack propagation and complete unloading (average of five samples, crack path shown as an arrow).
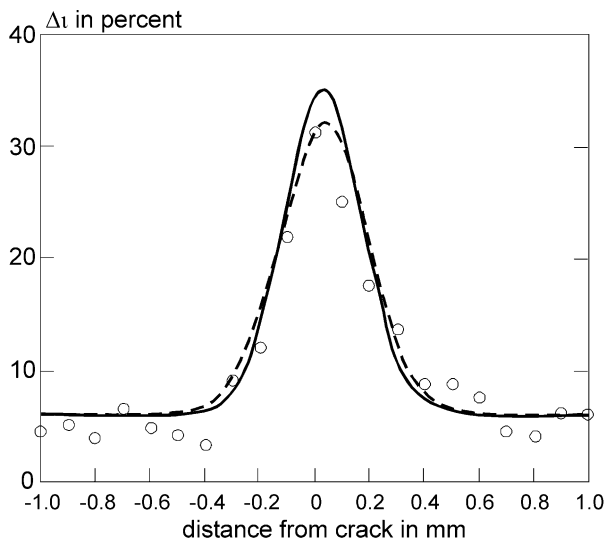

Fig. 17. $\Delta\iota$-Distributions transverse to the ligament (x-distribution at $y = 0.7$ mm in Fig. 14), (○) observed, - - - - Fit, ——deconvoluted distribution $\Delta\iota°$.

0.2 mm behind the crack tip. Here the plastic strain is about 6.5×10^{-4}. The critical stress for domain switching could be obtained from the experiments under load to be 15–20 MPa. The process zone height h is 0.29 mm, Young's modulus $E = 60000$ MPa and Poisson's ratio $\nu = 0.3$. Using these values a rise of the R-curve can be calculated to be $\Delta K_{I,calc} = 0.35 \pm 0.09$ MPa m$^{1/2}$ which is in good agreement with $\Delta K_{I,obs} = 0.39 \pm 0.03$ MPa m$^{1/2}$ (Fig. 10).

The relationship $l \approx 5\,h$ between rise distance of the R-curves l and process zone height h found in ZrO$_2$-ceramics can not be found for the investigated ferroelastic material, as the rise distance is 400 μm and the process zone height is about 300 μm.

Table 1
Residual stresses of sample U-Da2 in MPa, crack starts at $x = 0$, $y = 0.2$ mm and ends at $y = 0.8$ mm (marked by bold numbers)

	x-Direction				
y-Direction	−0.6 mm	−0.3 mm	0 mm	0.3 mm	0.6 mm
0.2 mm	−3±7	−7±8	**9±3**	4±4	−4±4
0.5 mm	−2±5	4±4	**0±4**	−4±4	−2±7
0.8 mm	−4±7	1±3	**1±5**	−7±5	−1±5
1.1 mm	−11±7	4±3	5±4	−2±6	1±4
1.4 mm	2±4	0±5	−1±3	−4±4	0±5

5. Summary

Microdiffraction analysis and fracture mechanical studies of Soft-PZT "PIC 151" were carried out and permitted a quantitative assessment of the size of the process zone, the inelastic strain due to domain switching and the associated stress. The development of an in situ bending device allowed the direct combination of microdiffraction and fracture mechanical experiments. The R-curve behavior of the investigated material is strongly influenced by the ferroelastic character. The distinct rise of the R-Curve is mainly based on domain switching processes. The tensile loading stresses cause domains oriented perpendicular to the stress to switch into a parallel orientation. This reduces the acting stress intensity and thus partially shields the crack tip. The rise of the R-curves could be calculated from the process zone height and the domain switching processes $\Delta\iota$ with sufficient consistency to the observed values. No residual stresses caused by domain switching could be proved. Since the ferroelastic domain switching is not

irreversible the shielding effect of domain switching on the process zone degrades partially if the sample is unloaded. As a consequence the plateau value of the R-curve can only be reached after running through the R-curve once again. As the process zone is not completely degraded after unloading, the rise distance is distinctly shorter.

Acknowledgements

References

1. Endriss, A., *Reorientierungsverhalten von Domänen und mikroskopische Gitterdeformation in piezoelektrischen PZT-Keramiken.* UFO Dissertation Bd. 302, Stuttgart, 1996.
2. Endriss, A., Hammer, M and Hoffmann, M. J., In-situ Untersuchungen des intrinsischen Piezoeffektes an PZT-Keramiken mittels Synchrotronstrahlung. Institut für Keramik im Maschinenbau, Universität Karlsruhe, Jahresbericht, 1997.
3. Li, S., Bhalla, A. S., Newnham, R. E., Cross, L. E. and Huang, C.-Y., 90° domain reversal in $Pb(Zr_xTi_{1-x})O_3$. *J. Mater. Sci.*, 1994, **29**, 1290–1294.
4. Ogawa, T. and Yamada, A., Ferroelectric domain-controlled ceramics. *Key Eng. Mater.*, 1999, **157–158**, 81–88.
5. Zhong, W. L., Wang, Y. G., Yue, S. B. and Zhang, P. L., Domain reorientation by poling of PZT ceramics in the morphotropic phase boundary region. *Solid State Communications*, 1994, **90**(6), 383–385.
6. Mehta, K. and Virkar, A. V., Fracture mechanisms in ferroelectric-ferroelastic lead zirconate titanate (Zr:Ti=0.54:0.46) ceramics. *J. Am. Ceram. Soc.*, 1990, **73**(3), 567–574.
7. Meschke, F., Kolleck, A. and Schneider, G. A., R-curve behaviour of $BaTiO_3$ due to stress-induced ferroelastic domain switching. *J. Eur. Ceram. Soc.*, 1997, **17**, 1143–1149.
8. Munz, D. and Fett, T., *Mechanisches Verhalten keramischer Werkstoffe: Versagensablauf, Werkstoffauswahl, Dimensionierung.* Springer Verlag, Berlin, Heidelberg, New York, 1989.
9. Evans, A. G., *Fracture in Ceramic Materials.* Noyes Publications, Park Ridge, New Jersey, 1984.